Electronic Supplementary Information (ESI)

Achieving High Capacity Organic Cathode FeF_3@$Li_2C_6O_6$/rGO Based on Interface Control Strategy

*Chengyi Lu ,[ac] Chen Dong ,[a] Haitao Wu ,[a] Dan Ni ,[a] Wang Sun ,[a] Zhenhua Wang [*ab] and Kening Sun[*ab]*

[a] *Beijing Key Laboratory for Chemical Power Source and Green Catalysis, School of Chemistry and Chemical Engineering, BIT-QUB Joint Center on Novel Energy and Materials Research, Beijing Institute of Technology, Beijing, 100081, People's Republic of China.*

[b] *Collaborative Innovation Center of Electric Vehicles in Beijing, No. 5 Zhongguancun South Avenue, Haidian District, Beijing, 100081, People's Republic of China.*

[c] *Shannxi Applied Physics and Chemistry Research Institute, Xi'an, 710061， People's Republic of China.*

[*] *E-mail: bitkeningsun@163.com, Email: 04710@bit.edu.cn*

Experimental

Materials synthesis

Φ The synthesis of cuboid-shape $Li_2C_6O_6$[1-3]

3g of commercial rhodizonic acid dihydrate ($H_2C_6O_6 \cdot 2H_2O$, 98%; Alfa) and 0.713 g of lithium carbonate (Li_2CO_3, >99%; Aladdin) were mixed in a mortar. Deionized water (40 mL) was added slowly to the mixture and stirred for 12 h. After the solution was centrifuged for 5 min at 12000 rpm, the precipitated powder was rinsed with ethyl alcohol (40 mL) and dried in a vacuum oven for 12 h. The obtained powder was heated at 200℃ under an argon (Ar) atmosphere for 17 h to obtain the final product.

②The synthesis of FeF_3@$Li_2C_6O_6$/rGO

Ⅰ The synthesis of spherical-shape $Li_2C_6O_6$

3g of commercial rhodizonic acid dihydrate ($H_2C_6O_6 \cdot 2H_2O$, 98%; Alfa) were added to deionized water (40 mL) to form mixture A; 0.713 g of lithium carbonate (Li_2CO_3, >99%; Aladdin) were added to deionized water (20 mL) to form mixture B. The mixture B was added slowly to the mixture A and stirred for 36 h. After the solution was centrifuged for 5 min at 12000 rpm, the precipitated powder was rinsed with ethyl alcohol (40 mL) and dried in a vacuum oven for 12 h. The obtained powder was heated at 200℃ under an argon (Ar) atmosphere for 17 h to obtain the final product.

Ⅱ The synthesis of $Li_2C_6O_6$/rGO

2g spherical-shape $Li_2C_6O_6$ were slowly added to the deionized water (40 mL) to form transparent mixed solution. Then 200 mg rGO were slowly added to the transparent mixed solution with ultrasound 3 h and stirred for 18 h. The mixture were poured into ethanol (600 mL) and stirred for 4 h. Finally, the ethanol mixture was distilled under low pressure and dried in a vacuum oven for 12 h at 30℃ to obtain the product $Li_2C_6O_6$/rGO.

Ⅲ The synthesis of FeF_3@$Li_2C_6O_6$/rGO

The obtained $Li_2C_6O_6$/rGO (500 mg) was slowly added to ethanol (200 mL) and stirred for 12 hours to form the mixture C. Then FeF_3 (7.5 mg) was dissolved in ultrapure water at 80

℃ and stirred for 2 h to form mixture D. Finally, the mixture D was added slowly to the mixture C and stirred for 12 h. After the solution was centrifuged for 5 min at 12000 rpm, the precipitated powder was rinsed with acetone (50 mL) and dried in a vacuum oven for 12 h to obtain the final product.

Sample characterization

The crystal structure of $Li_2C_6O_6$, $Li_2C_6O_6$/rGO and FeF_3@$Li_2C_6O_6$/rGO were characterized by X-ray diffraction (XRD). The morphology of $Li_2C_6O_6$, $Li_2C_6O_6$/rGO and FeF_3@$Li_2C_6O_6$/rGO were examined by scanning electron microscopy (SEM, QUANTA FEG 250). Transmission electron microscopy (TEM) images were obtained using a JEOL JEM-2100F. X-ray photoelectron spectroscopy (XPS) was employed by Physical Electronics 5400 ESCA. TGA thermal analyses were performed with TG/DTA6200 instrument at a rate of 10℃/min under nitrogen. Cyclic voltammetry (CV) was carried out between 2.0 and 4.5 V by a CHI660E electrochemical station.

Electrochemical measurements

According to the positive active material FeF_3@$Li_2C_6O_6$/rGO: acetylene black: polyvinylidene fluoride (PVDF) at a weight ratio of 8:1:1 in NMP (N-methyl pyrrolidone, 99%) which was used as solvent to make a slurry. Then the slurry was pasted onto the aluminium foil and dried under vacuum for about 12 hours at 100℃. The lithium metal anode was used as negative electrode, and the electrolyte consists of 1mol/L, LiPF6 and EC (ethylene carbonate) +DEC (Diethyl carbonate) +DMC (dimethyl carbonate) (volume ratio 1:1:1). The membrane is Celgard2400 microporous polypropylene film. A 2025 button Battery cells were assembled in an argon-filled glovebox with oxygen and water content below 0.5 p.p.m. The cLFP@SP discharge/charge tests were conducted at various rates within a voltage window from 1.5 to 3.5 V (vs Li^+/Li) on the BTS battery testing system (Landian, Wuhan, China). The Cyclic voltammetry (CV) measurements were performed using the same cell configuration with potential galvanostatic tests in the voltage range from 1.5 V to 3.5 V at a scan rate of 0.1 mV s^{-1}.

We have controlled the weight of active material on each electrode between 0.708 to 0.7965 mg/cm^2.

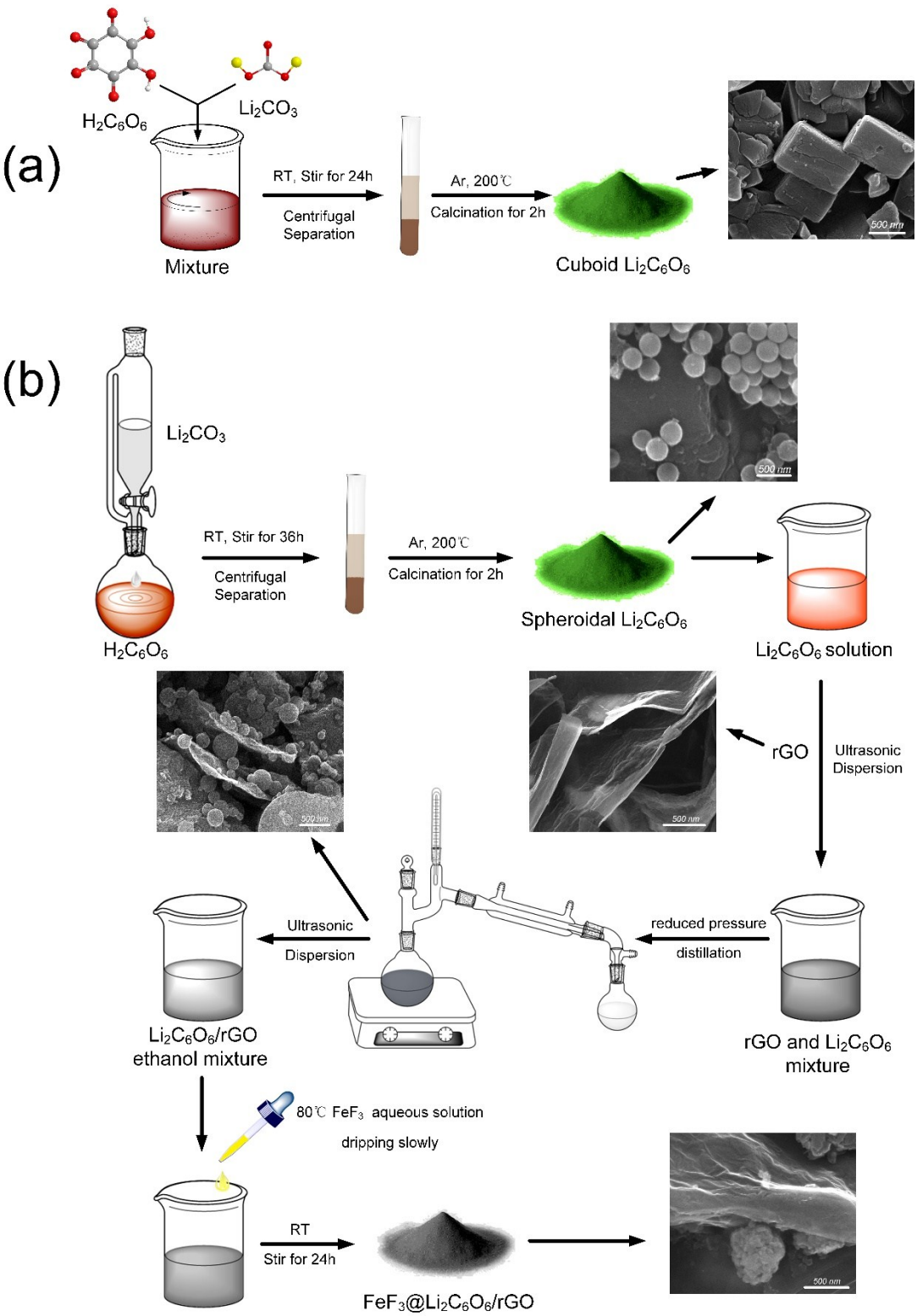

Fig. S1 The synthetic route: (a) the synthesis of cuboid-shape $Li_2C_6O_6$; (b) The synthesis of FeF_3@$Li_2C_6O_6$/rGO

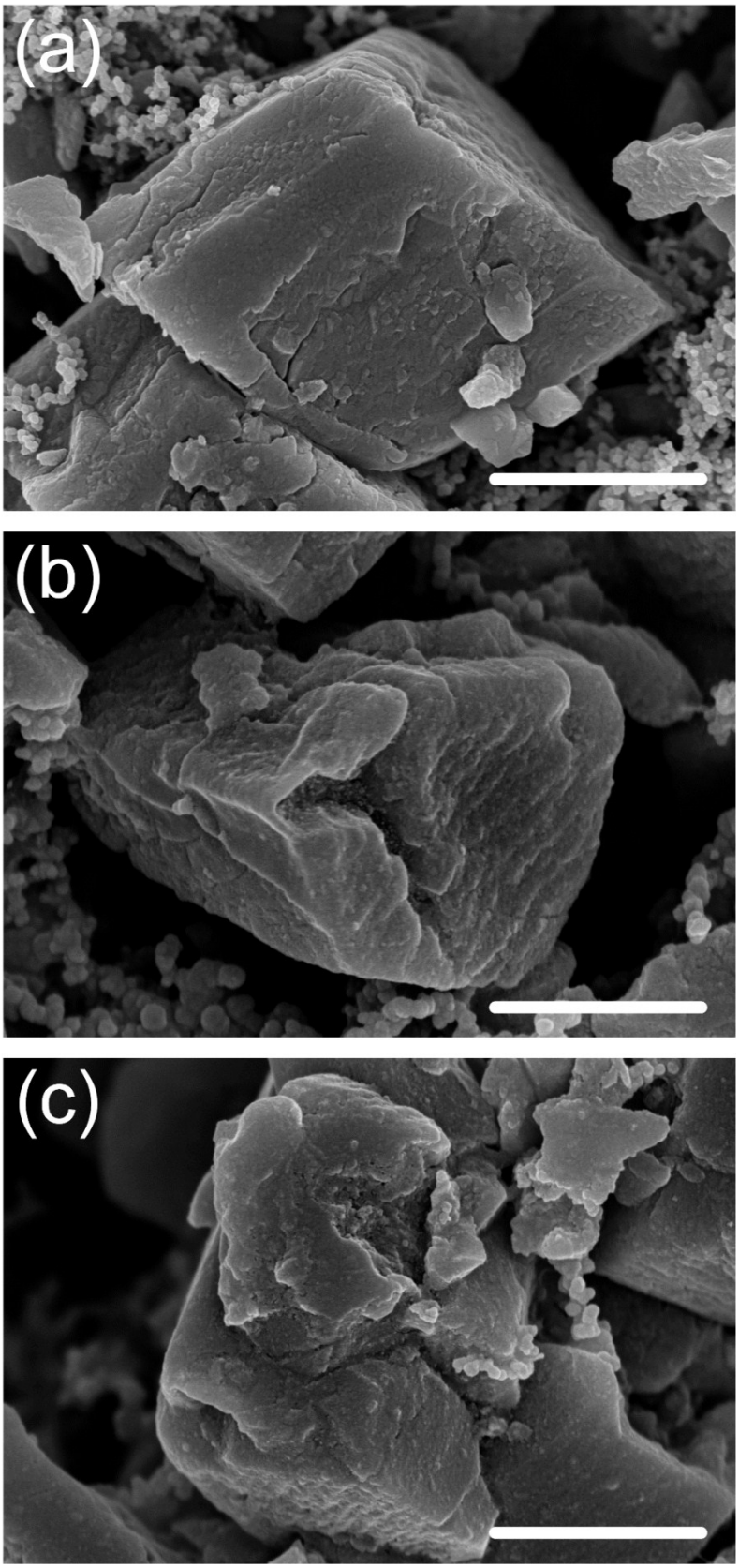

Fig. S2 The SEM image of cubes $Li_2C_6O_6$ after 1st, 50th and 100th charge/discharge cycle. Scale bar is 500 nm.

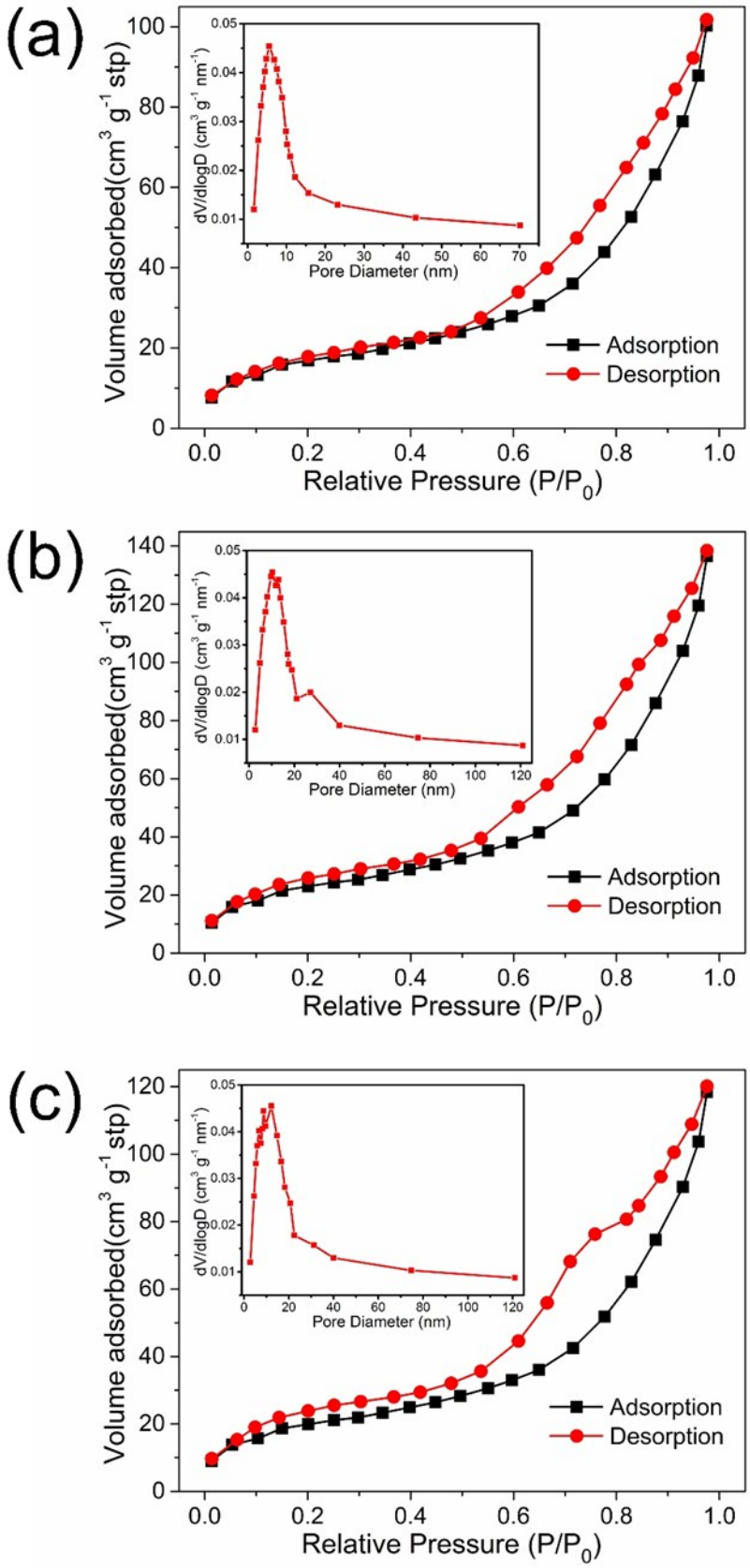

Fig. S3 Nitrogen adsorption−desorption isotherms and pore size distribution: (a) $Li_2C_6O_6$; (b) $Li_2C_6O_6$/rGO; (c) FeF_3@$Li_2C_6O_6$/rGO

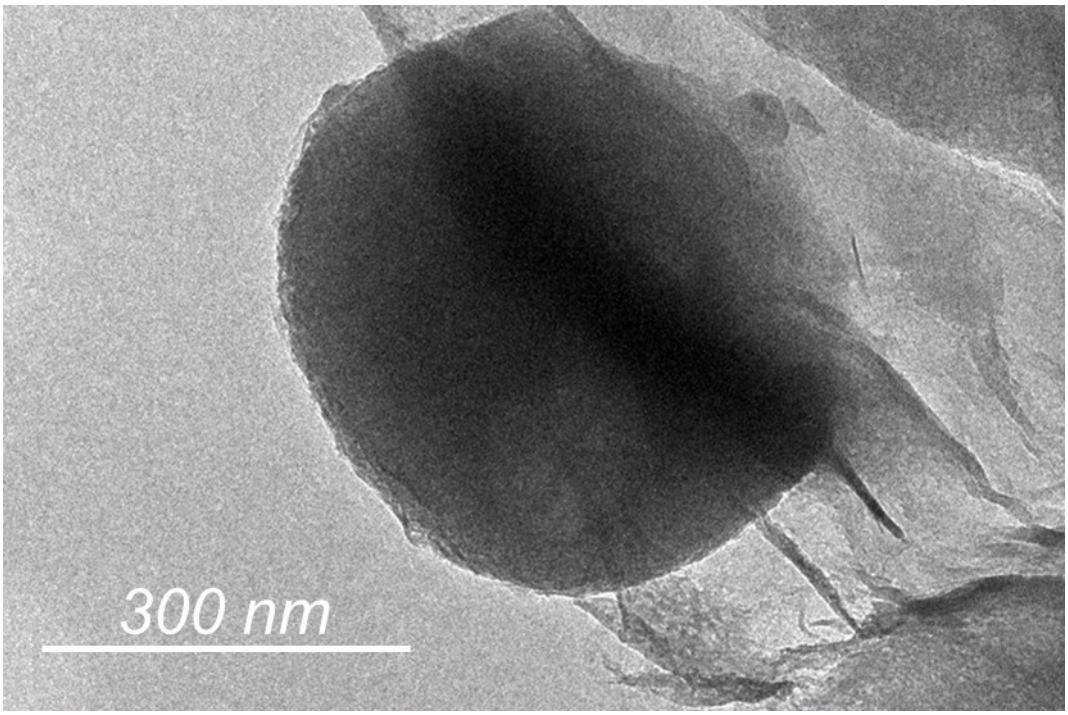

Fig. S4 The TEM image of $Li_2C_6O_6$/rGO

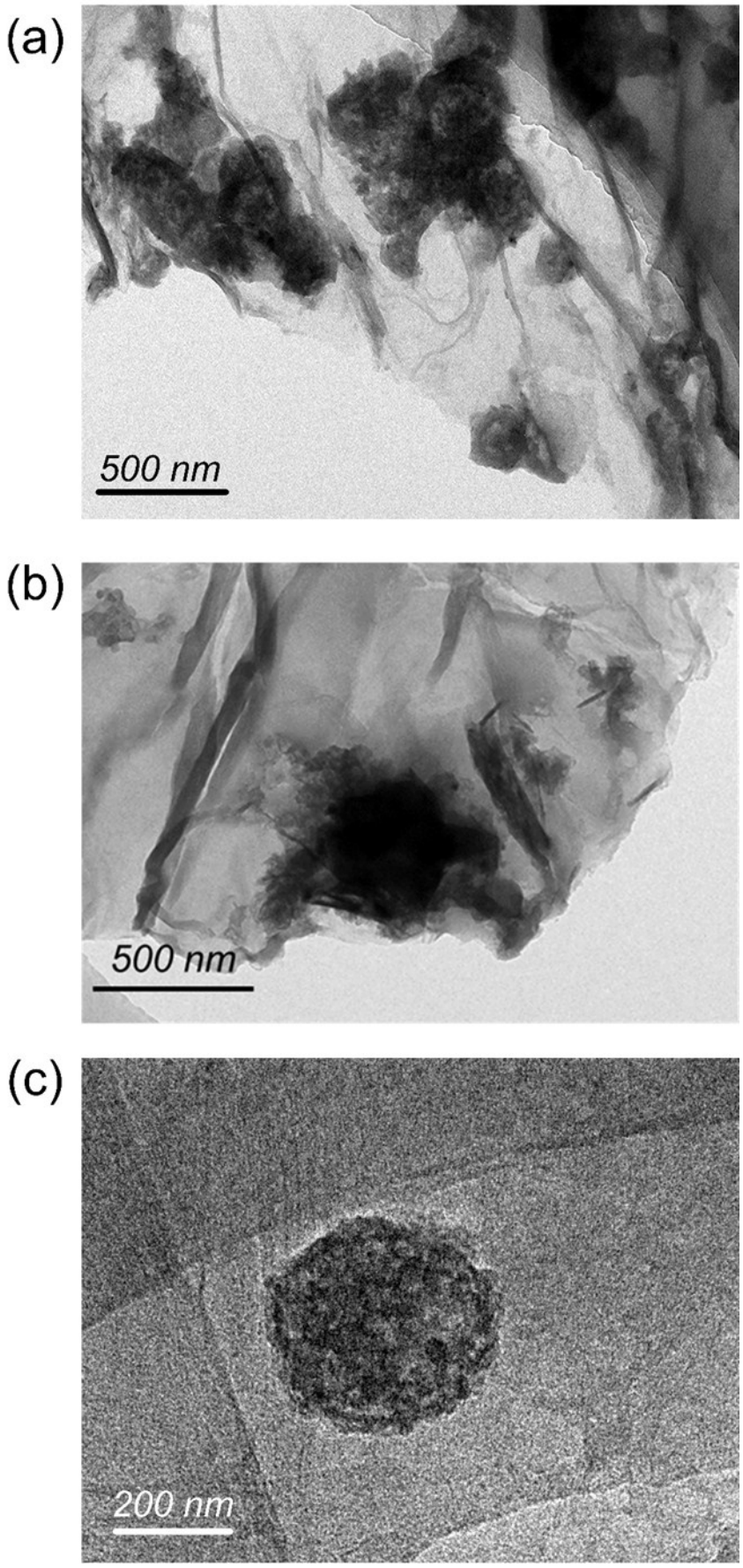

Fig. S5 The HRTEM image of FeF_3@$Li_2C_6O_6$/rGO

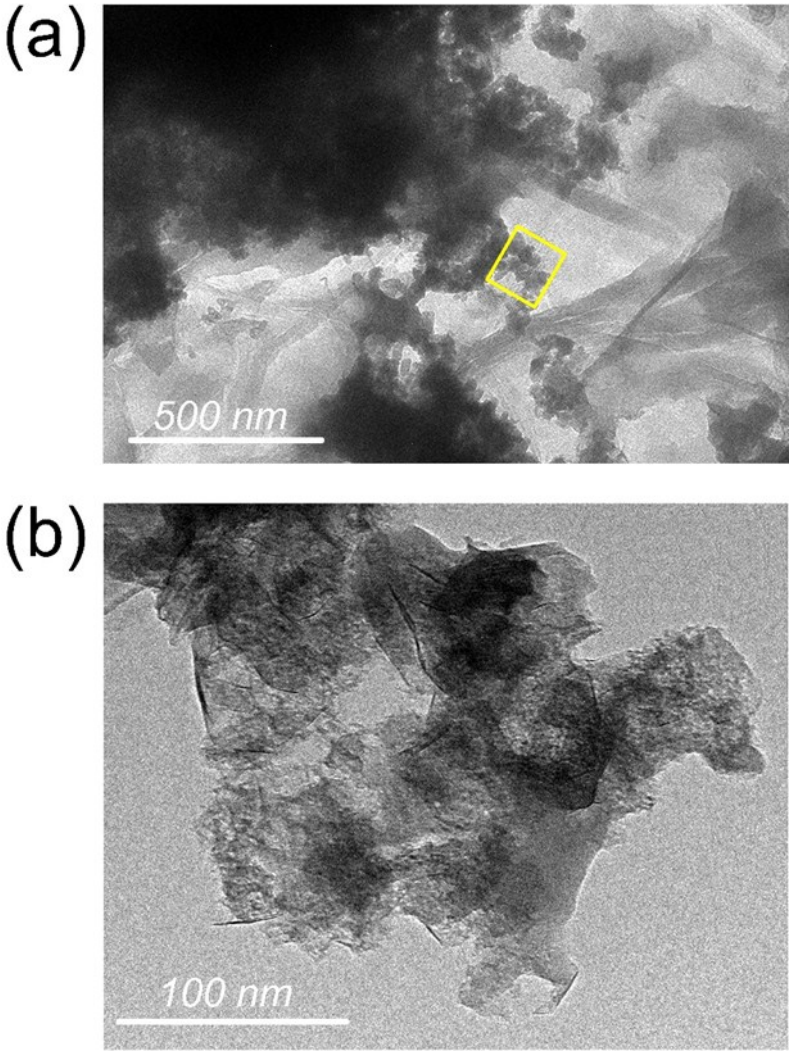

Fig. S6 The HRTEM image of FeF_3@$Li_2C_6O_6$/rGO: (b) shows the enlarged morphology of the selected region in (a) marked with a yellow box.

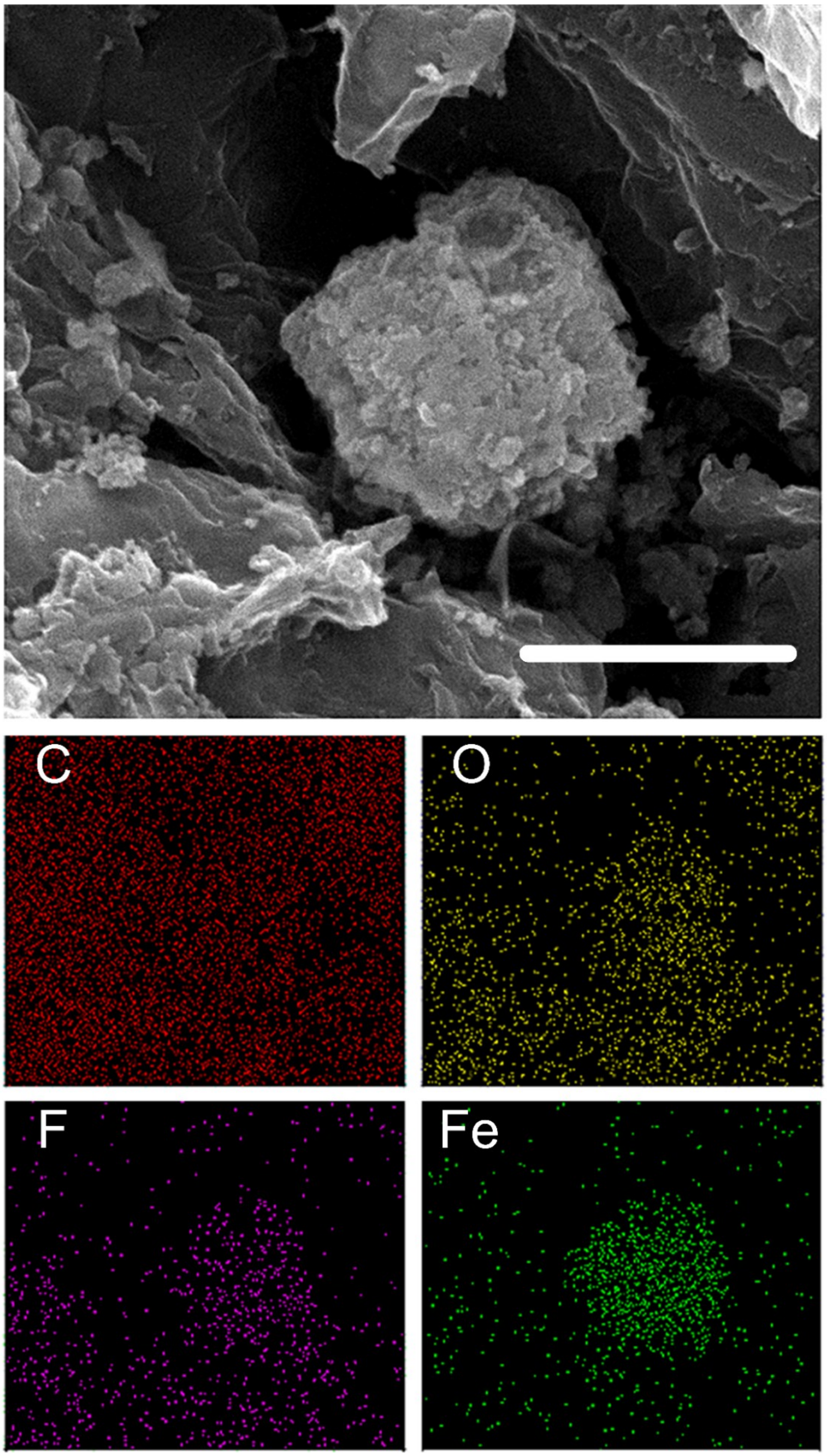

Fig. S7 The SEM and EDS mapping images of the FeF_3@$Li_2C_6O_6$/rGO. Scale bar is 500 nm.

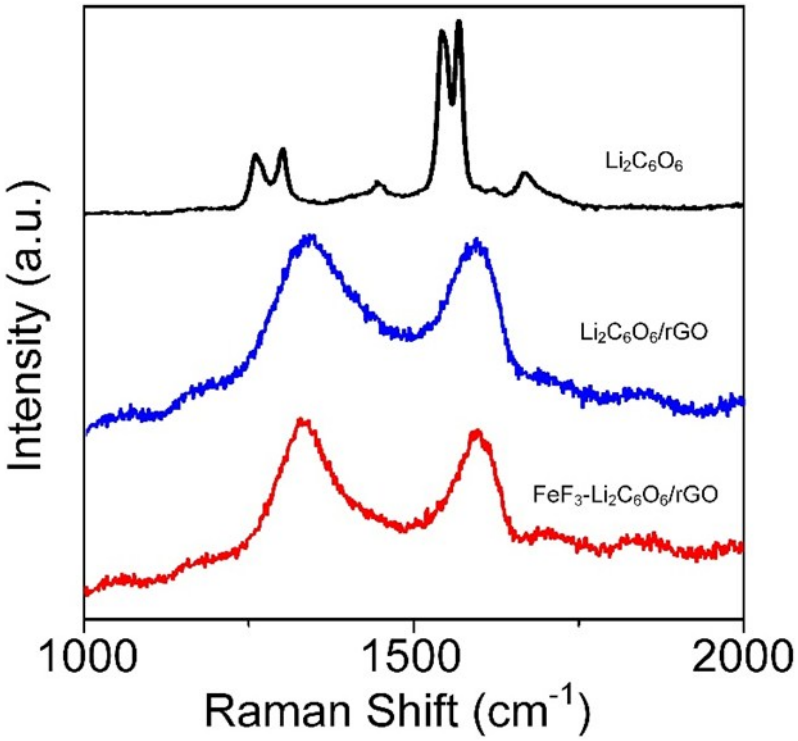

Fig. S8 The Raman spectra of $Li_2C_6O_6$, $Li_2C_6O_6$/rGO and FeF_3@$Li_2C_6O_6$/rGO at 1000~2000 cm^{-1}.

$Li_2C_6O_6$ has two obvious double peaks at 1250 cm^{-1} and 1550 cm^{-1}, respectively. However, due to the presence of rGO, $Li_2C_6O_6$/rGO and FeF_3@$Li_2C_6O_6$/rGO show obvious two peaks at 1343 cm^{-1} (D-band) and 1596 cm^{-1} (G-band), respectively.

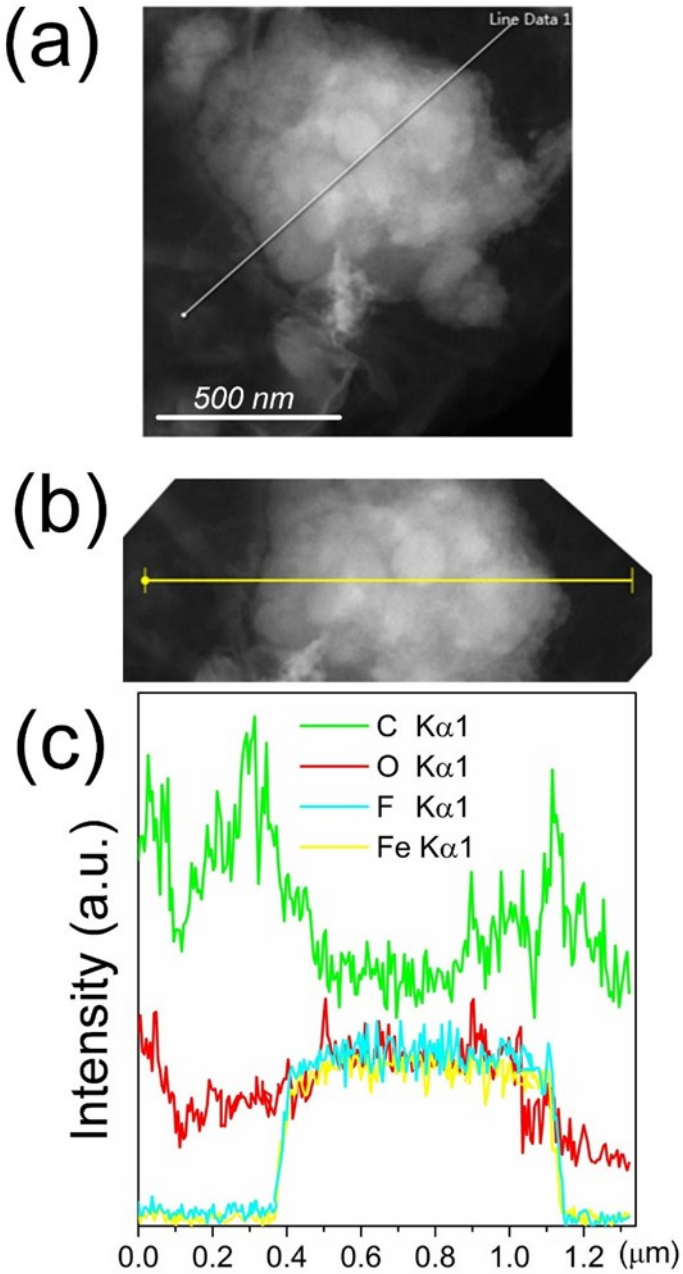

Fig. S9 The EDS mapping and line-profile of FeF_3@$Li_2C_6O_6$/rGO.

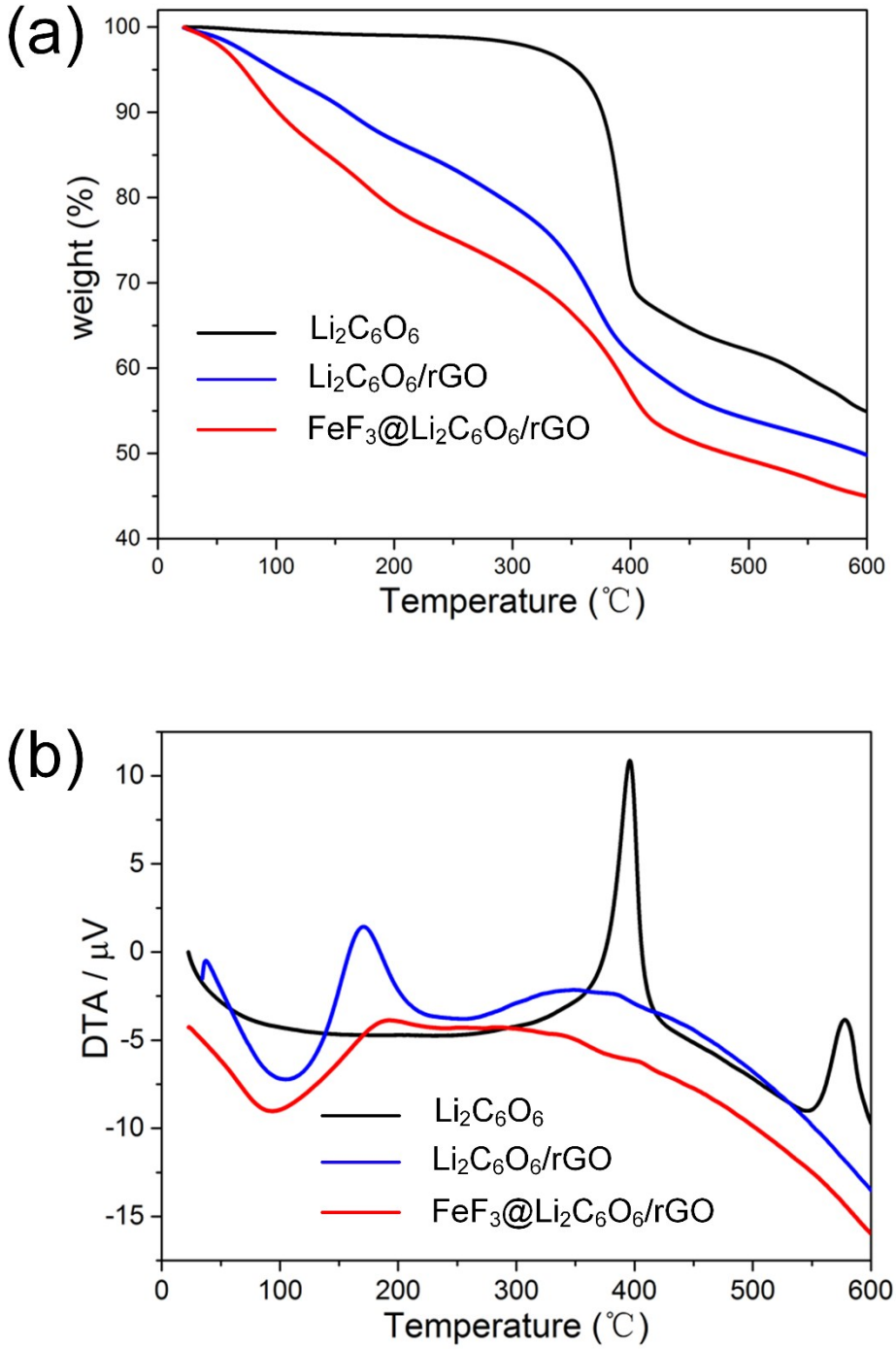

Fig. S10 (a) The TG of $Li_2C_6O_6$, $Li_2C_6O_6$/rGO and FeF_3@$Li_2C_6O_6$/rGO; (b) The DTA of $Li_2C_6O_6$, $Li_2C_6O_6$/rGO and FeF_3@$Li_2C_6O_6$/rGO. Heating rate of 10.0 K min^{-1}, Nitrogen atmosphere .

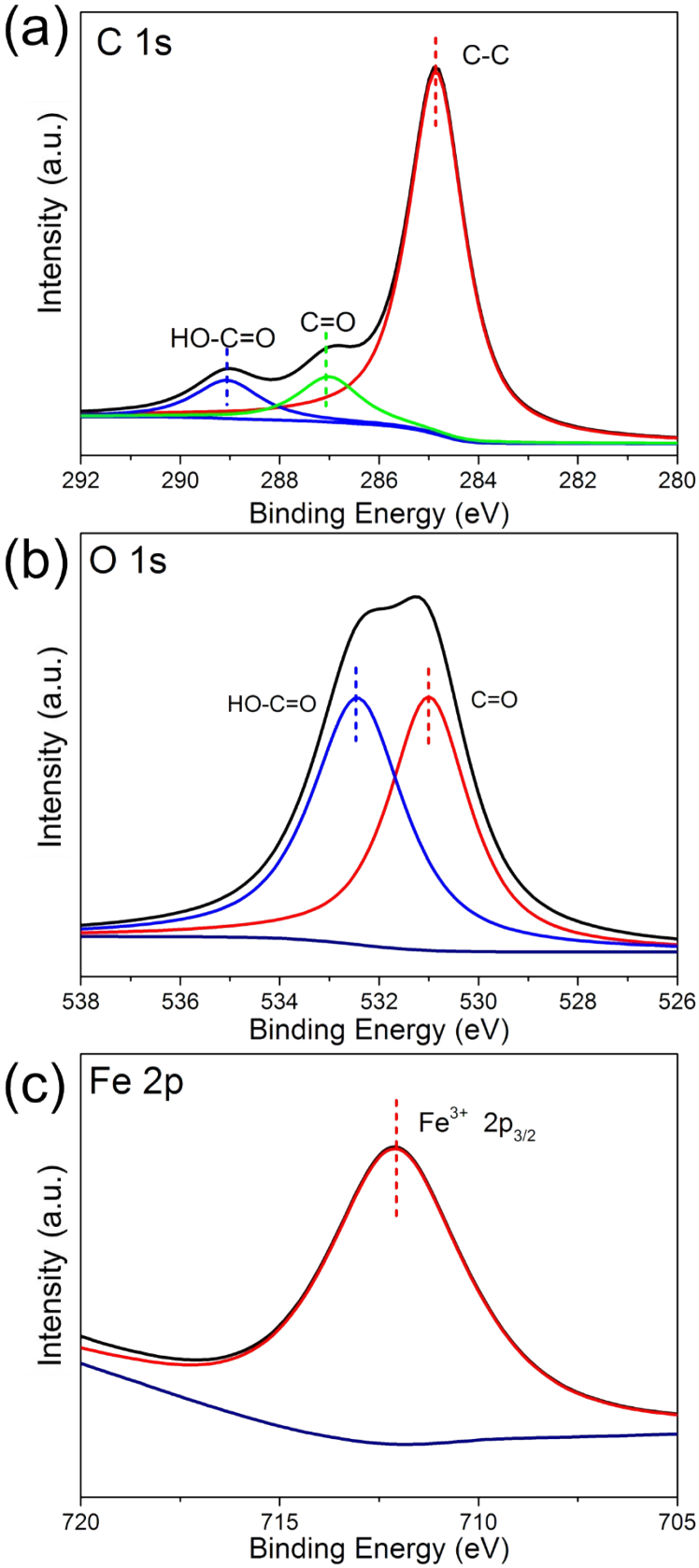

Fig. S11 The XPS spectrums of FeF_3@$Li_2C_6O_6$/rGO: (a) C 1s spectrum, (b) O 1s spectrum and (c) Fe 2p spectrum.

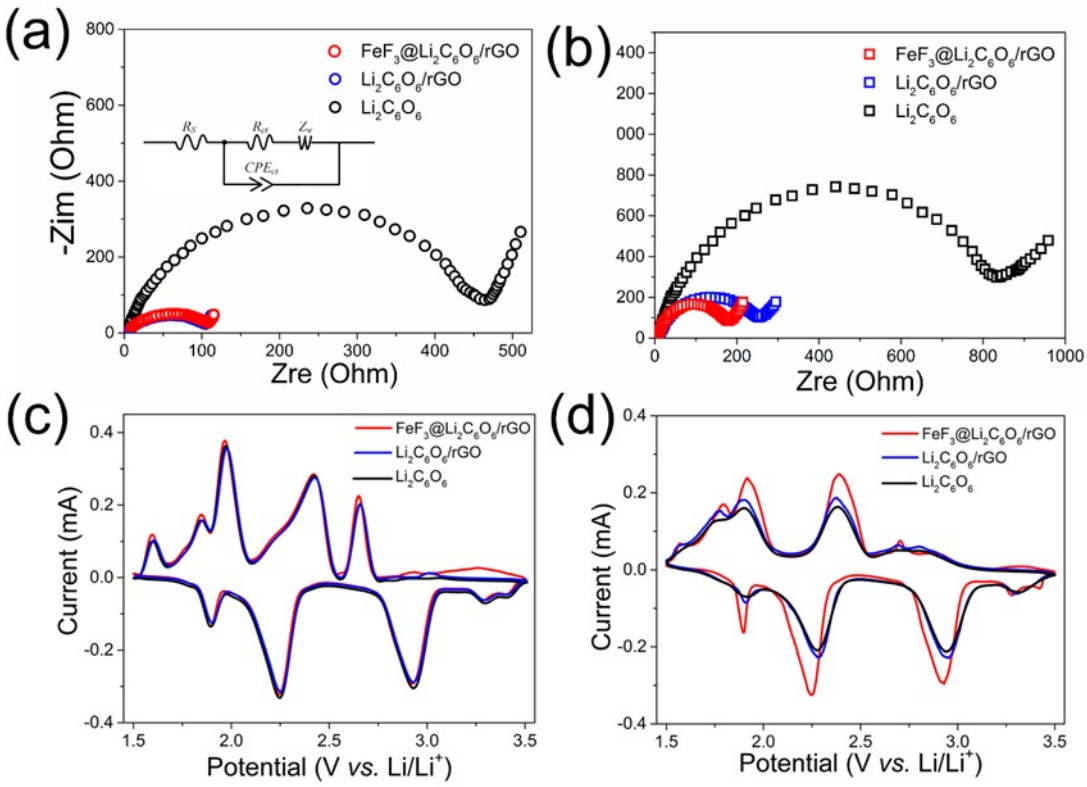

Fig. S12 (a)-(b) Electrochemical impedance spectroscopy (EIS) results of $Li_2C_6O_6$, $Li_2C_6O_6$/rGO and FeF_3@$Li_2C_6O_6$/rGO after 1st and 10th cycle; (c)-(d) Cyclic voltammetry curves of $Li_2C_6O_6$, $Li_2C_6O_6$/rGO and FeF_3@$Li_2C_6O_6$/rGO at 1st and 10th cycle, 0.1 mV.

Table S1 The typical fitted parameters in the electrochemical impedance spectroscopy

Samples	R_S /Ω	R_{ct} /Ω	R_{tol} /Ω	σ / (S·m^{-1})
$Li_2C_6O_6$	4.37	4686	6556.73	0.1350×10^{-3}
$Li_2C_6O_6$/rGO	3.98	252	339.68	2.6050×10^{-3}
FeF_3@$Li_2C_6O_6$/rGO	4.02	366	419.32	2.1106×10^{-3}

(The thickness of electrode coating is 100 μm and electrode surface area is 1.13 cm^2. $\sigma = l/RS$)

The conductivity of these materials by fitting the equivalent circuit of electrochemical impedance spectroscopy.[12, 13] R_s is the resistance of the electrolyte; R_{ct} and CPE_{ct} are the chargetransfer resistance and double-layer capacitance, respectively; Z_w is the Warburg impedance related to the diffusion of lithium ions into the bulk electrodes.[14,15] The conductivity of $Li_2C_6O_6$ is 0.1350×10^{-3} S/m, due to the existence of rGO, the conductivity of $Li_2C_6O_6$/rGO and FeF_3@$Li_2C_6O_6$/rGO is 2.6050×10^{-3} and 2.1106×10^{-3}, respectively. The conductivity of FeF_3@$Li_2C_6O_6$/rGO is close to commercial cathode materials.[16]

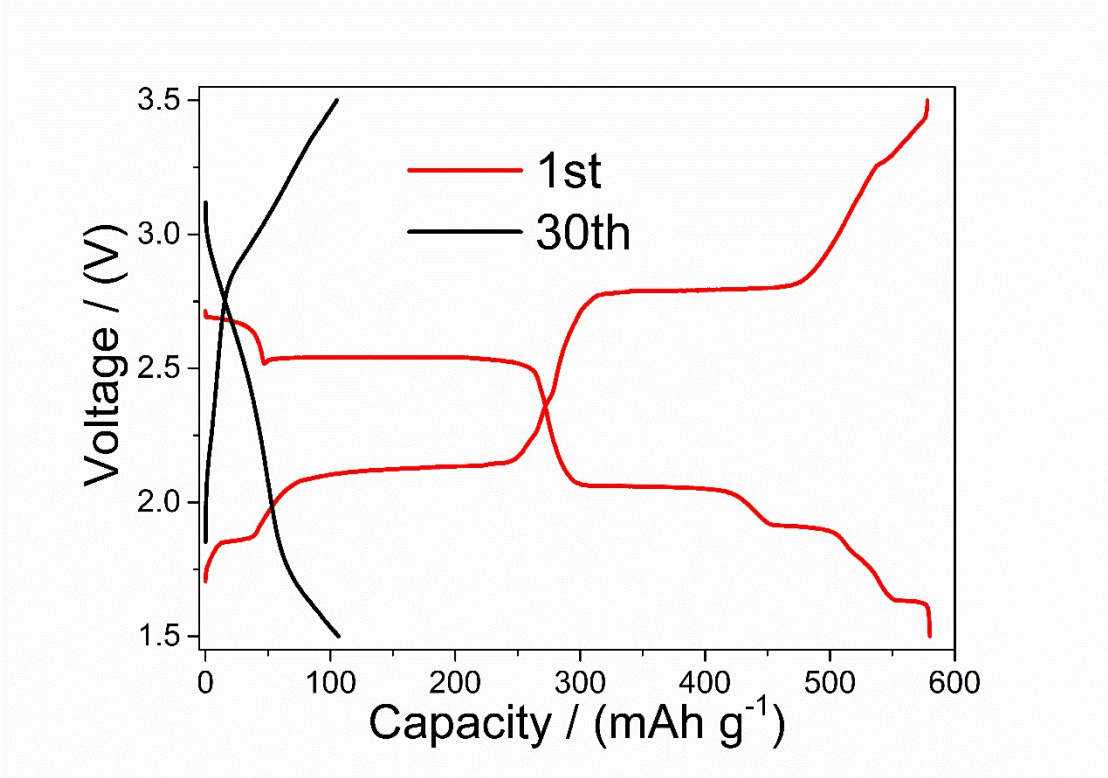

Fig. S13 The charge and discharge curves of cuboid $Li_2C_6O_6$ at 0.1C with initial and 30th cycyle (the specific capacity is about 520 mAh g^{-1} based on the weight of the whole electrodes).

Table S2 The comparison of different cathode material performance

Cathode materials	Discharge voltage /V	Specific capacity (mA h/g)	Cycle performance (after 100 cycles)
$LiCoO_2$ [17,18]	4.0	274	135
$LiFePO_4$ [19]	3.45	170	156
$Li_{1+x}Ni_{0.8-x}Co_{0.1+y}Mn_{0.1+z}O_2$ [20]	2.7-4.5	280	190
$Li_2C_6O_6$ [1-3]	2.7	590	320
THAQ [21]	2.8	148	35
PDBM [22]	3.0	150	135
PDAAQ [23]	2.5	221	140
PSCA [24]	2.0	287	169

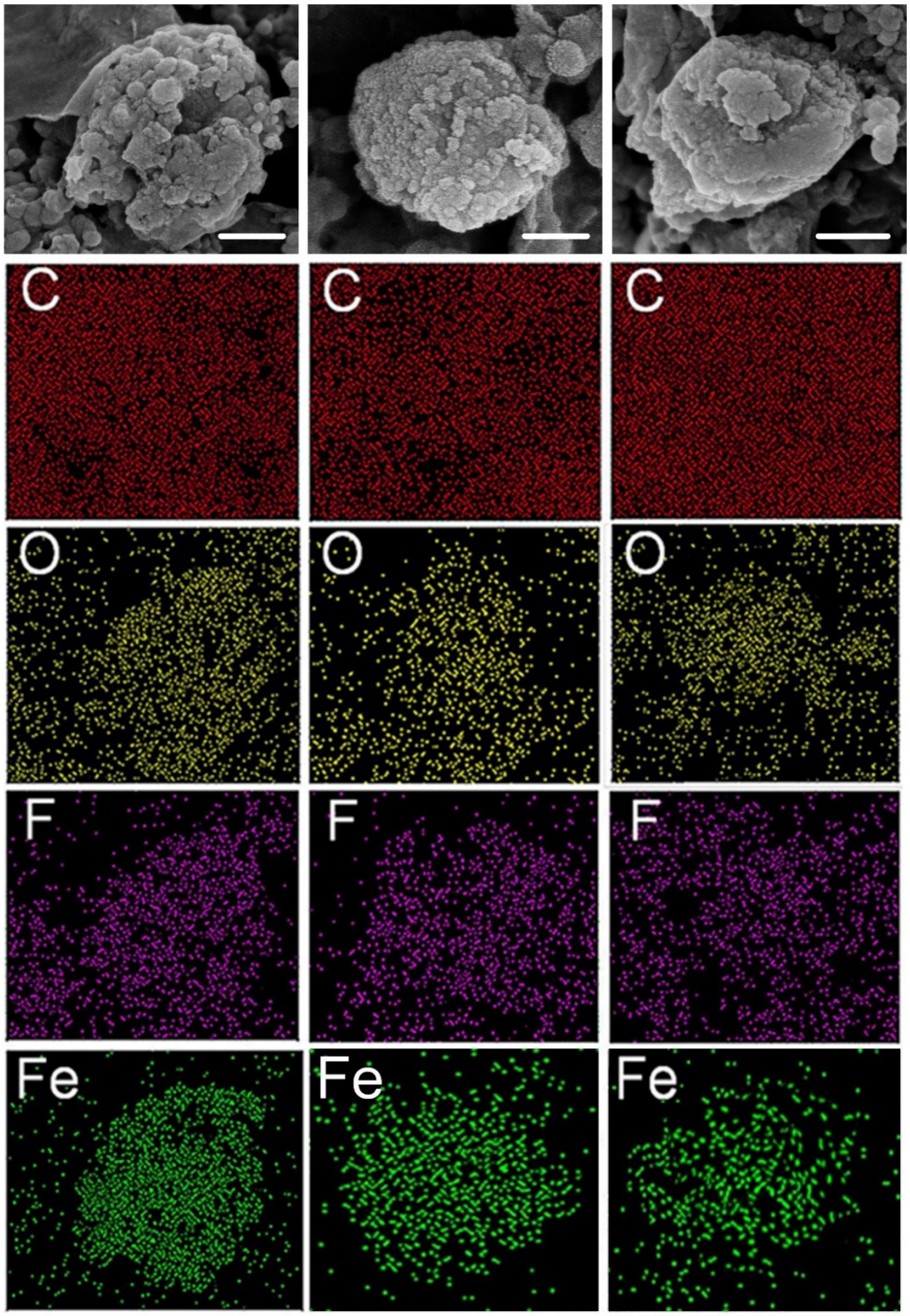

Fig. S14 The SEM images and EDS mapping images of the FeF_3@$Li_2C_6O_6$/rGO after 1st, 50th and 100th charge/discharge cycle. Scale bar is 200 nm

In Fig. 4, the morphologies were analysed by scanning electron microscopy (SEM) after the 1st, 50th and 100th cycles. In these SEM photos, we can find the changes in the particle size of $Li_2C_6O_6$, $Li_2C_6O_6$/rGO and FeF_3@$Li_2C_6O_6$/rGO three materials after the 1st, 50th and 100th cycles. The main reason for the capacity decay and poor cycling performance of $Li_2C_6O_6$ is flaking of the C_6O_6 layer and the increased surface area accelerating its dissolution in the electrolyte.[1] After 100th charge-discharge cycle, the particle size of $Li_2C_6O_6$ and $Li_2C_6O_6$/rGO become smaller due to the dissolution in the electrolyte, and the morphology of $Li_2C_6O_6$ and $Li_2C_6O_6$/rGO become irregular particles because of the flaking and dissolution of C_6O_6 layer (as shown in Fig. 4d-4i). Therefore, as the number of cycles increases, the C_6O_6 will dissolve and exfoliate more and more in FeF_3@$Li_2C_6O_6$/rGO. Due to the active coating formed on the surface of $Li_2C_6O_6$ is formed by crystallization of FeF_3, the active coating can slow the dissolution of $Li_2C_6O_6$ in the electrolyte (as shown in Fig. 4j-4l). As the number of cycle increases, more and more C_6O_6 will contact with the electrolyte and dissolve, eventually resulting in a decrease in capacity. However, there are many FeF_3 particles on the surface of $Li_2C_6O_6$ after 100th cycles, which proves that the FeF_3 has an inhibitory effect on the dissolution of $Li_2C_6O_6$.

References

[1] H. Chen, M. A. Dr, G. D. Prof, F. D. Dr, P. Poizot and J. M. T. Prof, *Chemsuschem*, 2008, **1**, 348-355.

[2] H. Chen, M. Armand, M. Courty, M. Jiang, CP. Grey, F. Dolhem, JM. Tarascon, PC. Poizot, *J. Am. Chem. Soc*., 2009, **131**, 8984-8988.

[3] H. Kim, D. H. Seo, G. Yoon, W. A. G. Iii, S. L. Yun, W. S. Yoon and K. Kang, *Phys. Chem. Lett.*, 2014, **5**, 3086-3092.

[4] Y. Liang , Z. Tao, J. Chen, *Adv. Energy Mater*., 2012, **2**, 742-769.

[5] K. Mizushima, P. C. Jones, P. J. Wiseman and J. B. Goodenough, *Mater Res Bull*., 1980, **15**, 783-789.

[6] L. X. Yuan, Z. H. Wang, W. X. Zhang, X. L. Hu, J. T. Chen, Y. H. Huang and J. B. Goodenough, *Energy Environ. Sci*., 2011, **4**, 269-284.

[7] Y. K. Sun, Z. H. Chen, H. J. Noh, D. J. Lee, H. G. Jung and Y. Ren, *Nat Mater*., 2012, **11**, 942-947.

[8] W. K. Wang, Y. Y. Zhang, A. B. Wang, Z. B. Yu, M. F. Han, Y. S. Yang, *Acta Phys.-Chim. Sin*, 2010, **26**, 47-50.

[9] T. L. Gall, K. H. Reiman, M. C. Grossel, J. R. Owen, *J. Power Sources,* 2003, **119**, 316-320.

[10] Z. Tang, G. X. Xu, *Acta Phys.-Chim. Sin*, 2003, **19**, 307-310.

[11] Z. Song, H. Zhan, Y. Zhou, *Chem. Commun*, 2008, **5**, 448-450.

[12] Q. Zhuang, J. Xu, X. Fan, Q. Dong, Y. Jiang, L. Huang and S. Sun, *Chinese. Sci. Bull.,* 2007, **52**, 1187-1195.

[13] L. Wang, J. Zhao, X. He and C. Wan, *Electrochim Acta*., 2011, **56**, 5252-5256.

[14] C. Wang, Z. Guo, W. Shen, Q. Xu, H. Liu and Y. Wang, *Adv. Funct. Mater.,* 2014, **24**, 5511–5521.

[15] D. Chao, C. Zhu, X. Xia, J. Liu, X. Zhang, J. Wang, P. Liang, J. Lin, H. Zhang, Z. X. Shen and H. J. Fan, *Nano Lett*., 2015, **15**, 565–573.

[16] P. P. Prosini, D. Zane and M. Pasquali, *Electrochim Acta*, 2001, **46**, 3517-3523.

[17] Y. Liang , Z. Tao, J. Chen, *Adv. Energy Mater*., 2012, **2**, 742-769.

[18] K. Mizushima, P. C. Jones, P. J. Wiseman and J. B. Goodenough, *Mater Res Bull*., 1980, **15**, 783-789.

[19] L. X. Yuan, Z. H. Wang, W. X. Zhang, X. L. Hu, J. T. Chen, Y. H. Huang and J. B. Goodenough, *Energy Environ. Sci*., 2011, **4**, 269-284.

[20] Y. K. Sun, Z. H. Chen, H. J. Noh, D. J. Lee, H. G. Jung and Y. Ren, *Nat Mater*., 2012, **11**, 942-947.

[21] W. K. Wang, Y. Y. Zhang, A. B. Wang, Z. B. Yu, M. F. Han, Y. S. Yang, *Acta Phys.-Chim. Sin*, 2010, **26**, 47-50.

[22] T. L. Gall, K. H. Reiman, M. C. Grossel, J. R. Owen, *J. Power Sources,* 2003, **119**, 316-320.

[23] Z. Tang, G. X. Xu, *Acta Phys.-Chim. Sin*, 2003, **19**, 307-310.
[24] Z. Song, H. Zhan, Y. Zhou, *Chem. Commun*, 2008, **5**, 448-450.